Gene Therapy (2003) 10, 1766–1775

www.nature.com/gt

RESEARCH ARTICLE

A model for the analysis of nonviral gene therapy

GA Banks[1], RJ Roselli[1], R Chen[1] and TD Giorgio[1,2]

[1]Department of Biomedical Engineering, Vanderbilt University, Nashville, TN, USA; and [2]Department of Chemical Engineering, Vanderbilt University, Nashville, TN, USA

Further understanding of the mechanisms involved in cellular and intracellular delivery of transgene is needed to produce clinical applications of gene therapy. The compartmental and computational model designed in this work is integrated with data from previous experiments to quantitatively estimate rate constants of plasmid translocation across cellular barriers in transgene delivery in vitro*. The experimental conditions between two cellular studies were held constant, varying only the cell type, to investigate how the rates differed between cell lines. Two rate constants were estimated per barrier for active transport and passive diffusion. Translocation rates of intact plasmid across the cytoplasmic and nuclear barriers varied between cell lines. CV1 cells were defined by slower rates (0.23 h^{-1} cytoplasmic, 0.08 h^{-1} nuclear) than those of the HeLa cells (1.87 h^{-1} cytoplasmic, 0.45 h^{-1} nuclear). The nuclear envelope was identified as a rate-limiting barrier by comparing the rate of intact plasmid translocation at each barrier. Slower intact plasmid translocation in CV1 cells was correlated with a reduced absolute capacity for transgene efficiency in comparison with HeLa cells. HeLa cells were three times more efficient than CV1 cells at producing green fluorescent protein per intact plasmid delivered to the nucleus. Mathematical modeling coordinated with experimental studies can provide detailed, quantitative understanding of nonviral gene therapy.*

Gene Therapy (2003) **10,** 1766–1775. doi:10.1038/sj.gt.3302076

Keywords: *plasmid quantitation; gene delivery; transgene expression; kinetic analysis; computational model*

Introduction

Gene therapy shows great promise in being an effective therapeutic strategy for human disease. In the past decade, excitement about gene therapy applications has stimulated numerous clinical trials using both viral and nonviral gene delivery techniques. Viral and nonviral delivery techniques have unique characteristics that have been studied extensively. The relative biological safety of nonviral gene delivery, as well as its transient property, has recently increased the interest of clinicians and scientists for application *in vivo*. Nonviral transfection is also cost-effective, easy to produce, and has few practical limitations in the size of the transgene, which are very promising features for *in vivo* applications.[1] Nonviral transfection, however, is limited by relatively inefficient transgene expression.

The key to improving the clinical outcomes of transfection with nonviral techniques includes optimizing the parameters involved in gene delivery and expression while maintaining the advantages of this method. Optimization depends critically on detailed understanding of the barriers to, and mechanisms of, DNA translocation in the cell. Initial enthusiasm for nonviral gene therapy in clinical applications had turned the attention to the clinic rather than focusing on the quantitative, basic science studies of the mechanisms involved. Quantitative and reproducible methods that can be disseminated and utilized by multiple investigators in the analysis of nonviral gene therapy are increasingly recognized for their significant role in producing the next generation of nonviral gene therapies.[2] Clear relations are needed to connect specific functional activities with the associated structural features of nonviral therapies.

The primary obstacles to nonviral transgene expression have been the focus of speculation by many, but rarely have these obstacles been evaluated in systematic detail.[3] *In vivo*, the first barrier the lipoplex encounters is the systemic barrier. This multifaceted barrier includes inactivation of lipoplex systemically and efficient delivery of transgene to the target cells. The next barrier is translocation through the target cell to the nucleus for transcription and gene expression. The work presented in this paper focuses on *in vitro* gene delivery at the cellular level while preserving characteristics required for safe *in vivo* gene therapy.

Once the lipoplex has reached a target cell, translocation through intracellular barriers is necessary to facilitate transgene expression (Figure 1). These barriers include (1) binding of the lipoplex to the cell surface; (2) entry of the lipoplex into the cells; (3) lipoplex escape from the endosome, if endocytosis was the entry pathway; (4) lipoplex dissociation to release intact plasmid DNA; (5) transport through the cytosol to the nucleus; and (6) entry into the nucleus.[4] Intracellular inactivation of the plasmid, potentially mediated by factors that include low pH exposure and DNAse activity,[5] is an additional obstacle to transgene expression.

The rate-limiting steps in lipoplex/plasmid translocation have not been well characterized. Presumably, the nuclear envelope and transport through the nuclear pore

Correspondence: Dr TD Giorgio, Department of Biomedical Engineering, Vanderbilt University, Box 351620, Station B, Nashville, TN 37235, USA
Received 13 October 2002; accepted 10 April 2003

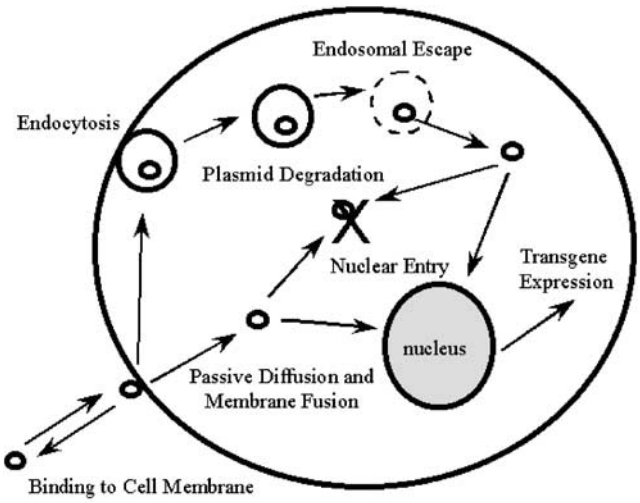

Figure 1 *The cellular steps of lipid-mediated gene delivery.*

complex play critical roles in transgene expression. Thus, the nuclear barrier may be a key rate-limiting step in nonviral transgene expression.[6] Other possible rate-limiting steps include endosomal escape and unidentified methods of plasmid degradation in the cytoplasm during trafficking to the nucleus.[7,8] However, few systematic and quantitative studies have been conducted to identify the mechanisms of gene translocation to the nucleus or to characterize the most important rate-limiting steps in expression.

Previous 'optimizing' efforts have generally modulated one parameter of transgene delivery to identify a local maximum in transgene expression. These maximization efforts offer a satisfactory platform for studies that explore relative comparisons of parameter modulation on gene expression. However, individual parameter maximization provides little information regarding the global intracellular obstacles to transgene efficiency and, generally, cannot be directly compared to other studies. Many intracellular events that control transgene expression may be modulated by a single parameter. For example, addition of a nuclear localization signal (NLS) on the lipoplex may facilitate nuclear entry while simultaneously modulating cytoplasmic delivery or endosomal escape due to NLS-related changes in size/charge. Identification of rate-limiting steps allows for improvement in nonviral gene expression by focusing on knowledge of the events that control the desired transgene expression. This can be done by understanding the mechanisms of translocation and optimizing the passage of these barriers rather than maximizing expression by modifying a single parameter, as has been done in the past.

Many mechanisms of transgene delivery have been developed utilizing both physical and biochemical methods. Physical methods include ballistics (the 'gene gun'),[9] electroporation,[10] ultrasound,[11] hydrodynamic pressure changes,[12] and jet injection.[13] Biochemical delivery methods such as lipid formulations, cationic lipid chemistry,[14,15] DNA condensation, addition of glycosylated moieties,[16] and use of synthetic peptides to act as NLSs have also been studied. The cellular mechanisms of these delivery methods are, generally, not well understood, and the fate of the plasmids has also not been comprehensively quantified or evaluated.

In vitro, different cell lines yield a wide range of transgene efficiency when treated under identical transfection conditions.[17] This implies that there may be a role for intracellular properties as a modulation of transgene expression. Casual observation, for example, suggests a significant role for the nuclear barrier in controlling transgene expression as mitotic cells generally express more transgene product than slowly dividing cells.[18] Other studies have evidence supporting plasmid translocation across the nuclear membrane as a critical obstacle through characterization of the relation between transgene expression and mitosis by modulating cell cycle timing.[19] The implication is that plasmid transport into the nucleus is facilitated by barrier changes during mitosis. These and other observations are extremely useful in understanding the mechanisms of transgene expression, but lack the systematic and quantitative approach necessary to rationally design and evaluate nonviral delivery systems with improved function.

Previous work proposed a model of plasmid transport that considered the successful navigation at each barrier to transgene expression.[20] The purpose was to characterize the rates of various intracellular mechanisms and processes involved in transgene delivery and expression in order to optimize the therapeutic potential of the nonviral gene therapy. The compartment model of Ledley and Ledley[20] included a mathematical representation based on biological half-lives and rate constants. The primary limitation of this work was the lack of appropriate experimental data on nonviral gene delivery at that time.

New methods now allow detailed measurements that characterize plasmid delivery and translocation in cellular systems. One group has extended the notions of Ledley and Ledley[20] with the additional feature of an integrated approach using experimental data and computational modeling to identify the effects of changes in the delivery system on plasmid delivery rates.[21] This group proposed a detailed model that required the use of data obtained from other laboratories, using a variety of experimental conditions and cell lines. The considerable potential power of this approach was limited by the assumptions intrinsic to the use of experimental data derived from a variety of sources. The study concluded that it is possible to predict the effect of parameter changes on expression and the dependence of these changes on rate constants. Two different analyses were performed, using rates obtained from previous work and their own experimental data. One consequence of this approach is the need to presume that the same rate constants equally characterize different cell lines. Cell lines, however, have been shown to have varying capacities for transgene expression, complicating the application of 'universal' intracellular rate constants. A similar complication to the interpretation is the use of rates from different experimental arrangements to form a single representation. Clearly, modeling must be conducted with experimental data sets that are appropriate and compatible. Current research needs to include further investigation of the mechanisms of gene delivery, including identification of rate-limiting steps in delivery,

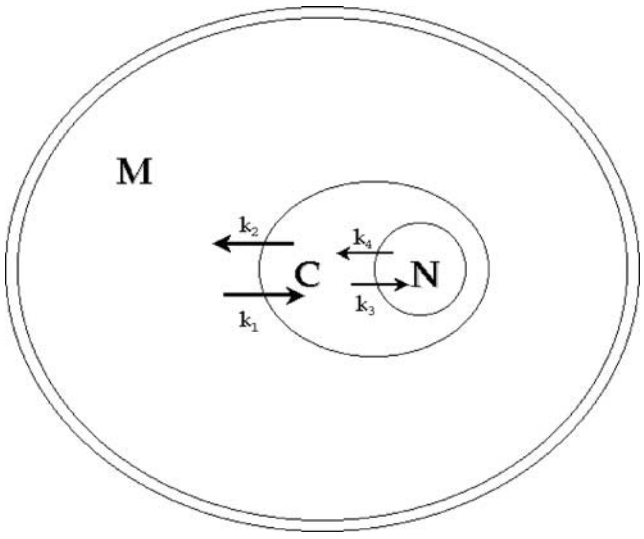

Figure 2 *The compartmental model. A cellular representation of the compartmentalization where M is the extracellular medium compartment, C is the cytoplasm, and N is the nucleus. The k_i variables are the rate constants: k_1 governs movement into the cell, k_2 governs transport out of the cell, k_3 governs transport into the nucleus, and k_4 governs movement out of the nucleus.*

as well as a quantitative method to compare the results of different experimental systems.

The current work extends that of others[20,21] by providing an integrated approach matching mathematical modeling to available experimental data. This work uses a mathematical representation based on a compartmental model (Figure 2) and complimentary experimental data to characterize and analyze intracellular mechanisms in nonviral gene therapy. A model was developed with three compartments that reflect important biological functions in nonviral gene therapy. A mathematical representation of this compartmental model was utilized to evaluate quantitative data acquired from previous experiments performed in our laboratory.[22] These data conform to the physical and mathematical models to estimate the relative significance of specific intracellular mechanisms. Rate constants derived from our analysis of experimental data are used to characterize the mechanism/s that are responsible for heterogeneous capacity for transgene expression in two *in vitro* cell types, HeLa cells (human epitheliod, ATCC CCL-2) and CV1 cells (monkey fibroblast, ATCC CCL-70), and to identify possible rate-limiting steps during transgene delivery.

Results

HeLa cells

Data from previous nonviral gene therapy experiments were used to estimate the rate of plasmid translocation across HeLa cell barriers in an *in vitro* system.[22] Experimental details are described previously[22] and are not reproduced here. Techniques and nomenclature particularly germane to this work are highlighted in the Methods section that follows the Discussion. Evaluation of the following results depends on a clear understanding of the corresponding mathematical models. Development of these models is detailed in the Methods portion of this work. The comparison of model prediction with experimental results for apparent plasmid delivery is shown in Figure 3. Figures 3a, b, and c show the change in equivalent plasmid number over time in the medium, cytoplasm, and nucleus, respectively. The relative magnitude of plasmid equivalents among

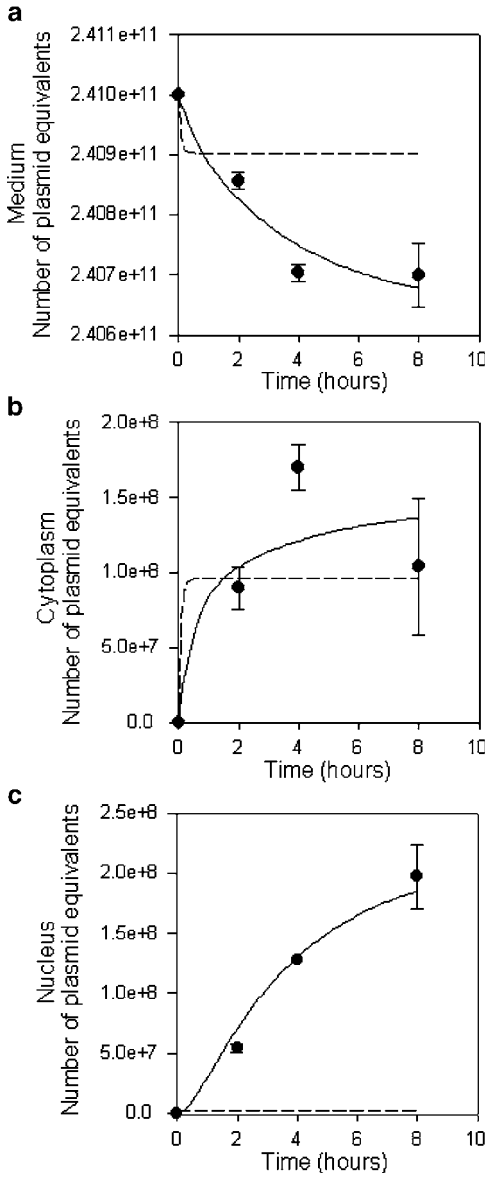

Figure 3 *Model and experimental data for HeLa cells. The points on graphs (b) and (c) are experimental results measured at time 0, 2, 4, and 8 h after addition of lipoplex.[22] The initial conditions were M(t=0)=2.41E+11, C(t=0)=0, and N(t=0)=0. The points on graph (a) were calculated from the initial condition minus the total intracellular plasmid obtained from multiplying the number of treated cells with the sum of the experimental results of graphs (b) and (c). The dashed lines are model predictions considering only passive diffusion as a transport mechanism. The solid lines represent model prediction of plasmid number equivalents based on the rate constants estimated from the final mathematical model that includes both active and diffusive transport. (a) Number of plasmid equivalents in the extracellular fluid (medium), (b) the cytoplasm, and (c) the nucleus. Experimental data are mean values with standard deviations for n=4 experiments.*

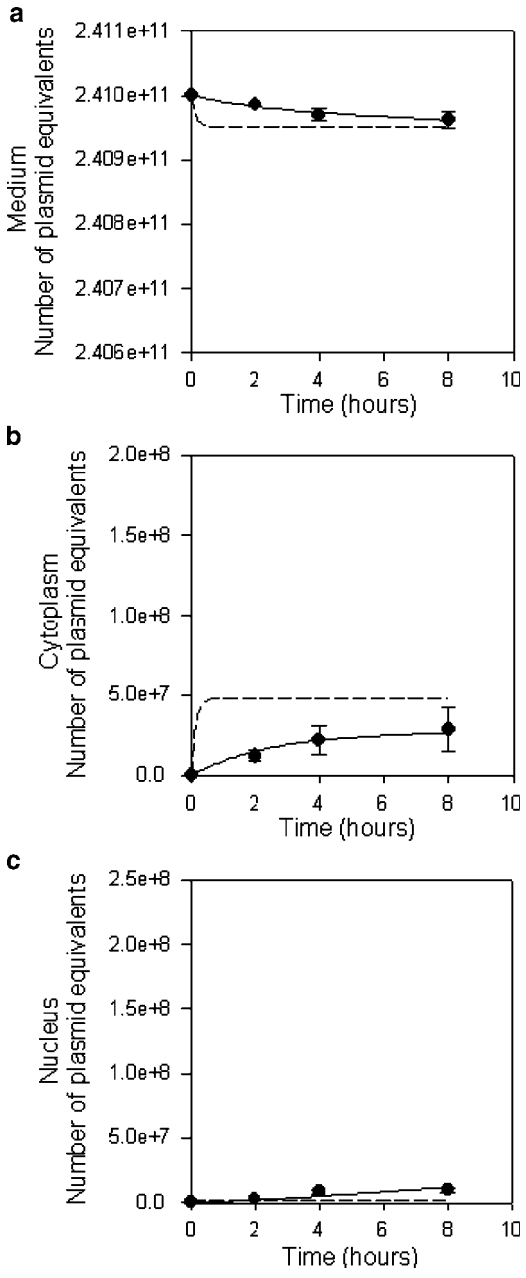

Figure 4 *Model and experimental data for CV1 cells. The points on graphs (b) and (c) are experimental results measured at time 0, 2, 4, and 8 h after addition of lipoplex.[22] The initial conditions were M(t=0)=2.41E+11, C(t=0)=0, and N(t=0)=0. The points on graph (a) were calculated from the initial condition minus the total intracellular plasmid obtained from multiplying the number of treated cells with the sum of the experimental results of graphs (b) and (c). The dashed lines are model predictions considering only passive diffusion as a transport mechanism. The solid lines represent model prediction of plasmid number equivalents based on the rate constants estimated from the final mathematical model that includes both active and diffusive transport. (a) Number of plasmid equivalents in the extracellular fluid (medium), (b) the cytoplasm, and (c) the nucleus. Experimental data are mean values with standard deviations for n=4 experiments.*

compartments reflects, in part, the difference in compartment volumes.

The dashed lines in Figures 3 and 4 represent the passive diffusion portion of the mathematical model. Passive diffusion, clearly, did not accurately reflect the dynamic behavior of the experimental data, so active transport was incorporated into the mathematical model. The final model behavior of plasmid transfer, represented by the solid lines in Figure 3, is characterized by the rate constants (Table 3) numerically estimated using Equations (1)–(3). These rates can be mathematically manipulated to gain additional understanding of cellular transport mechanisms for plasmid DNA. Conversion into volumetric rate constants was performed as described and resulted in values also shown in Table 3.

Further manipulation of these delivery rates can yield mechanistic insight. Active transport and passive diffusion are both potential contributors to the transport of fluorescently labeled, plasmid DNA nucleotides across the cellular barriers and are characterized by the rate constants in Table 4. The conversion of rate constants to reflect active and passive transport was performed using Equations (11) and (14). The active transport rate constant across the medium/cytoplasm (*mc*) barrier was positive, implying net import of plasmid DNA nucleotides into the cell cytoplasm ($k_{act}^{mc} = 0.63\ h^{-1}$). The passive diffusion rate constant across the same barrier was twice the value of the active rate constant and also positive ($k_{diff}^{mc} = 1.24\ h^{-1}$).

The positive rate constants for the cytoplasm/nucleus (*cn*) barrier transport imply net apparent plasmid delivery to the nucleus from the cytoplasm. The much larger active rate constant ($k_{act}^{cn} = 36.4\ h^{-1}$, $k_{diff}^{cn} = 0.45\ h^{-1}$) suggests that Cy3-fluorescence associated with plasmid DNA nucleotides enters the nucleus predominantly via active transport, whereas plasmid nucleotide translocation across the cellular membrane was primarily via passive diffusion. This result is an important focus of the Discussion.

CV1 cells

The same compartmental model analysis was applied to another experimental system to quantitatively compare rate constants in gene delivery as a function of cell type. Experimental measurements of apparent plasmid delivery to an epithelial cell line (CV1) that has a lower capacity for nonviral gene expression than HeLa cells were analyzed. The experimental conditions were held constant; only the cell type (HeLa *versus* CV1) was modulated between the two sets of experimental transfections.

The experimental data and model results for the CV1 cell studies are shown in Figure 4. Figure 4a shows the apparent plasmid number in the extracellular medium as a function of time and Figures 4b and c show the apparent plasmid number in the cytoplasm and nucleus compartments, respectively. The corresponding rate constants estimated using the compartmental model for CV1 cells and further equations are shown in Tables 3 and 4. The active rate across the *mc* barrier was negative ($k_{act}^{mc} = -0.11\ h^{-1}$) implying net export of plasmid, while the diffusive rate was positive ($k_{diff}^{mc} = 0.34\ h^{-1}$) across the same barrier. The sum of these rate constants is greater than zero, implying net fluorescent nucleotide accumulation in the cytoplasm, consistent with experimental observations. The positive rate constants for the *cn* barrier in CV1 cells ($k_{act}^{cn} = 5.15\ h^{-1}$, $k_{diff}^{cn} = 0.08\ h^{-1}$) continue to suggest that both transport techniques participate in apparent plasmid translocation into the nucleus. These estimated rates can be used to compare

among experiments to note the effects of experimental modifications.

Plasmid concentrations

Plasmid concentrations in the intracellular compartments were calculated by dividing the experimentally obtained apparent plasmid number by the corresponding compartment volume. (The volumes of the HeLa system were V_m=1.0E+3 μl, V_c=3.98E−1 μl, V_n=7.22E−3 μl. The volumes of the CV1 system were V_m=1.0E+3 μl, V_c=1.99E−1 μl, V_n=3.61E−3 μl.) Initial plasmid concentration added to the cells was obtained by spectrophotometry and spectrofluorescence as previously described.[22] The number of plasmids translocated from the supernate was calculated at any time as a difference between the starting plasmid number and the number of plasmids delivered intracellularly. In this way, the small reduction in extracellular plasmid can be determined with precision. There was no statistically significant diminution of the supernate plasmid concentration due to adsorption to the walls of an empty, control well. Fluorescence measurements of the lipoplex-containing cell culture medium were unchanged following 24-h incubation in a cell-free culture well.

The apparent plasmid concentrations are shown in Figure 5 as a function of compartment and time for both HeLa and CV1 cells. The intracellular plasmid equivalent concentrations generally increased over time. Interestingly, each compartment had a higher apparent plasmid concentration than the previous compartment.

The cytoplasmic plasmid equivalent concentration in the HeLa cells rose rapidly during the first 4 h with the corresponding apparent nuclear plasmid concentration maximum delayed until 8 h. Most striking was the greater magnitude of apparent plasmid concentration in the nucleus as compared to the cytoplasm. Also of note is that the extracellular medium compartment had the smallest concentration of plasmid equivalents after time zero. Observations in CV1 cells indicate that the medium compartment had a higher concentration than the cytoplasm until 8 h, reflecting the slower *mc* transport rate. The *cn* barrier, however, characterized the large active rate constant with the largest concentration over all time. The most obvious difference in apparent plasmid translocation between the two cell behaviors is that CV1 nuclei concentrations were lower than HeLa nuclei concentrations at all time points.

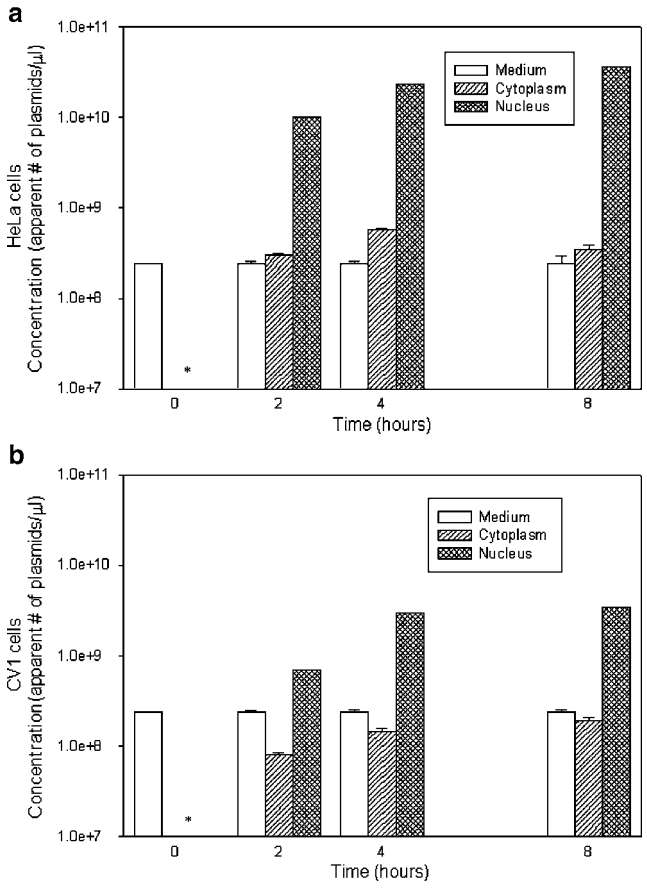

Figure 5 *Apparent plasmid concentration increase from extracellular medium to the nucleus. Apparent plasmid concentration data were calculated from experimental results by dividing the reported plasmid number in each compartment by the respective compartment volume.[22] The data for cytoplasm and nucleus were obtained by quantitative flow cytometry; the medium values were calculated from a mass balance on plasmid. The volumes were calculated from the measured diameters of the cells and nuclei or the added extracellular medium. (a) Apparent plasmid concentration in HeLa cell compartments. (b) Apparent plasmid concentration in CV1 cell compartments. Experimental data are mean values with standard deviations for n=4 experiments. *Values are zero for cytoplasm and nucleus.*

Discussion

Plasmid translocation rates in the HeLa cells

The rate constants obtained in this work are based on published experimental data interpreted through a biologically relevant compartmental model.[22] The rate-limiting barriers to nonviral gene therapy and the effects of modulated parameters such as cell type on plasmid translocation can be revealed through this quantitative approach.

Plasmid translocation into the nucleus of the HeLa cells appears to represent the fastest step in the cellular system (nuclear delivery rate=36.8 h^{-1}). This rate is 20 times faster than the plasmid delivery rate at the cell membrane (cytoplasmic delivery rate=1.87 h^{-1}). This observation would seem to contrast nonquantitative, previous nonviral gene expression experiments that suggested the nuclear barrier as one of the rate-limiting steps in cellular delivery.[6,17,23] The most probable interpretation of this result, however, is consistent with the previous work of others in identifying the nuclear membrane as a limiting obstacle to transgene expression in nonviral systems.

The rapid translocation of Cy3-fluorescence into the nucleus and against the concentration gradient is consistent with the hypothesis of intracellular plasmid degradation to oligonucleotides small enough to pass through the nuclear pore. Measurements of nuclear pore diameter range from 26 to 40 nm, with an outer diameter of 100–120 nm.[24–26] Oligonucleotides smaller than 68-mers have been shown to rapidly accumulate in the nucleus.[27] Previous work has revealed intracellular degradation of plasmid into oligonucleotides.[5] These oligonucleotides, due to their size, can then presumably be imported into the nucleus through the nuclear pore complex.

Supporting this interpretation is the overwhelming extent of active apparent plasmid transport into the nucleus (98.8%, *versus* 1.2% for passive transport), especially when compared to the estimated active transport across the cell membrane (33.5%, *versus* 66.5% for passive transport) obtained from the mathematical model estimations. In each case, the relative extent of active and passive transport is obtained from a comparison of the corresponding rate constants (Table 4). These new, quantitative features of plasmid transport are a direct product of the compartment model approach.

The plasmid used in the experimental work was labeled uniformly by guanidine conjugation chemistry (Mirus LabelIt kit, Panvera Corp., Madison, WI, USA). Thus, the fluorescence calibration reports the number of plasmid-derived base pairs, but cannot distinguish between intact, functional plasmid and oligonucleotide degradation products derived from the original Cy3-labeled plasmid. As a result, intranuclear Cy3 fluorescence intensity is converted to the number of full transcript plasmid equivalents and reported as either 'apparent plasmid' concentration or the number of 'plasmid equivalents'. The current hypothesis suggests that the level of Cy3-fluorescence in the nucleus is not an accurate measure of transcriptionally active plasmid DNA. In this case, current experimental evidence alone cannot characterize the role of the nuclear barrier as a rate-limiting step in the delivery of intact plasmid DNA into the nucleus. Additional experimental studies to evaluate this possibility are beyond the scope of the present computational study. Nevertheless, this contribution offers insight into the variability of previous measures of plasmid access to the nucleus. Photographic and biochemical evaluations of nuclear-delivered plasmid have produced inconsistent results among methods and studies. These measures might be productively re-evaluated with consideration of the present hypothesis of intracellular plasmid degradation and subsequent oligonucleotide transport.

Based on the lipoplex diameter and the nuclear pore dimensions and transport characteristics, intact plasmid is unlikely to be actively imported into the nucleus. If the active rate of transport into the nucleus is presumed to be predominantly the transport of oligonucleotides, then the transport of intact plasmid is presumably characterized by passive diffusion ($k_{diff}^{cn} = 0.45\ h^{-1}$). Lipid and lipoplex formulation provide significant protection against degradation of plasmid DNA,[5] implying that both active and passive transports through the *mc* barrier reflect cytoplasmic delivery of intact plasmid. Comparing the rates of functional plasmid transport across the barriers, the greatest obstacle is represented by the nuclear membrane (nuclear delivery rate=0.45 h^{-1}), rather than the cellular membrane (cytoplasmic delivery rate=1.87 h^{-1}).

Plasmid translocation rates in the CV1 cells

Analyzing the CV1 cell system as for HeLa cells, apparent plasmid translocation into the nucleus represents the fastest step in cellular transgene delivery (nuclear delivery rate=5.23 h^{-1}). This value is 26 times greater than the cytoplasmic delivery rate (cytoplasmic delivery rate=0.23 h^{-1}). These transport rates can be mathematically decomposed into active and passive characteristics. Active transport is 98% of the total delivery rate of Cy3-fluorescence into the nucleus ($k_{act}^{cn} = 5.15\ h^{-1}$) of CV1 cells, suggesting that only 2% of the nuclear fluorescence is contributed by intact plasmid. In contrast to HeLa cells, active lipoplex transport across the *mc* barrier of CV1 cells is negative ($k_{act}^{cn} = -0.11\ h^{-1}$), indicating active export of plasmid out of the cell. Active transport from the cytoplasm into the extracellular medium is a process functionally equivalent to exocytosis. Active exportation accounts for 35% of the total transport of plasmid equivalents across the *mc* barrier, leaving the other 65% of transport to passive import of apparent plasmid.

Measurements and rate constants reveal less apparent plasmid delivery in CV1 cells than HeLa cells, suggesting that CV1 cells have greater obstacles at both the *mc* and *cn* barriers. However, model and mathematical results provide the additional details to compare active transport *versus* passive transport for each barrier and cell line. The ratios of active transport to diffusive transport at each barrier are very different in both cell types. Active transport is responsible for 98% of apparent plasmid translocation through the nuclear barriers and 33–35% through the cytoplasmic barriers. Apparent plasmid translocation across CV1 cell barriers is not as rapid as for HeLa cells, but the proportion of active to passive transport is preserved across cell types. CV1 cells also appear to demonstrate a capacity for active export of internalized plasmid equivalents, a behavior not associated with HeLa cells (Table 4).

Transgene expression

Experimental measures of transgene expression were made simultaneously with measurements of apparent plasmid delivery.[22] These measurements represent the percent of the cell population that is producing green fluorescent protein (GFP), based on the fluorescence intensity measured by flow cytometry (percent positive). At 4 h, GFP expression in terms of percent positive in HeLa cells was double that of CV1 cells.[22] By the eighth hour after transfection, HeLa percent positive cells were nine times greater than CV1 percent positives. However, by the eighth hour, the ratio between the percent positive cells and the number of intact nuclear-associated plasmids in HeLa cells was three-fold greater than the comparable ratio in CV1 cells. Based on this observation, CV1 cells are less efficient than HeLa cells at producing GFP per intact plasmid delivered to the nucleus. HeLa cells, therefore, have more efficient intact plasmid delivery, translocation to the nucleus, and higher transgene expression than CV1 cells. There is the possibility that differences in transgene expression among cell types reflect cellular properties not explicitly modeled in this work rather than a relation to intranuclear intact plasmid delivery. Identification of the mechanism(s) responsible for the transgene expression efficiency in HeLa cells could be used to develop methods for boosting the expression efficiency in more clinically relevant systems.

Barriers to nonviral gene expression

The active and diffusive rate constants obtained from this coordinated approach can be used to compare experimental systems and techniques to identify rate-limiting steps. The effect of modulations designed to overcome those obstacles can also be assessed in future

work. Based on the hypotheses identified in this work, intact plasmid entry into the nucleus appears to be a rate-limiting step in nonviral gene expression. Nuclear translocation of intact plasmid is actually two to four times slower than cytoplasmic delivery of plasmid from the extracellular medium. These observations are consistent for two cell lines with significantly different capacities for nonviral gene expression, suggesting that absolute, not relative, delivery rates are critical factors controlling transgene expression in nonviral delivery systems.

The relative failure of a purely passive diffusion model to accurately represent plasmid transport to the cytoplasm reflects the well-known importance of endocytosis (and other active transport mechanisms) in transgene delivery. Perhaps of greater interest is the model prediction that active transport also contributes significantly to transnuclear delivery of apparent plasmid. Based on current understanding of nuclear transport, fluorescence in the nuclear compartment is likely to reflect oligonucleotides rather than intact plasmid. Nevertheless, the prediction of active plasmid transport into the nucleus, coupled with significant transgene expression, supports the presence of hypothetical active nuclear transporters of intact plasmid.

Model and experimental extensions

An extension of the current model with additional compartments and corresponding mathematics could allow estimation of rate constants for transgene expression from experimental data. Other new compartments could include cellular membrane binding (bilayer), endosomal escape, other barriers of cytoplasmic trafficking, and final transgene expression. The lack of suitable, comparable experimental data is the primary limitation on model extensions. Nonetheless, additional experimental measures would facilitate comparisons between additional compartments and treatments, providing more formal and robust correlation between plasmid delivery kinetics and transgene expression.

Methods

Data of James and Giorgio[22]

Plasmid DNA fluorescently labeled with Cy3 was formulated with cationic lipid to create lipoplexes that were added to cultured mammalian cells. Quantitative methods provided the fluorescence intensity per intact, 5 kb plasmid. Flow cytometry was used to measure the fluorescence intensity per cell and per isolated nucleus; calibration data were used to estimate intact plasmid number from measured fluorescence intensity. Clearly, 5 kb of oligonucleotides derived from degradation of the fluorescently labeled plasmid possesses, in sum, the same fluorescence intensity as a single 5 kb plasmid. For this reason, plasmid data from James and Giorgio[22] derived from fluorescence measurements are referred to as 'apparent plasmid' or 'plasmid equivalents' to clarify the possibility that some fluorescence is associated with oligonucleotides derived from plasmid DNA degradation rather than from intact, functional plasmid DNA.

Cellular compartmental model

A compartmental model was developed to reflect the physical organization of *in vitro* mammalian cell transfection experiments. This compartmental model was integrated with experimental analysis of plasmid delivery that had been measured in extracellular and natural, intracellular compartments. Transgene expression demands intact plasmid DNA transport from the extracellular medium, into the cell and, ultimately, the nucleus. The physical obstacles to nuclear entry include the outer, cellular membrane, trafficking through the cytoplasm to the nucleus, and entry to the nucleus through the nuclear envelope. Since the detailed characteristics of cytoplasmic trafficking are not yet understood, a model was developed that combines important, mechanistic events to yield measurable outcomes associated with transport across barriers: the cellular and nuclear membranes. Figure 2 illustrates the cellular compartmental model of a nucleated cell submerged in fluid medium.

The three-compartment model included the extracellular fluid or medium (M), the cell cytoplasm (C), and the cell nucleus (N). These compartments are critical in the understanding of key mechanisms of nonviral transgene expression. Previous experimental work in our laboratory measured intracellular plasmid delivery and apparent nuclear translocation of delivered plasmid in HeLa and CV1 cells over a 24-h period as a function of time.[22] Briefly, fluorescent plasmid was complexed with liposomes made of a 1:1 mole ratio of 1,2-dioleoyloxy-3-trimethylammonium-propane (DOTAP) and dioleoylphosphatidylethanolamine (DOPE) to form a cationic lipoplex. Quantitative analysis of plasmid number in the cell cytoplasm and nucleus was obtained using flow cytometry. The use of Cell Scrub™ eliminated outer membrane-associated plasmid on both the cell membrane and nuclear membrane.[22] All references to compartment-associated plasmids in this work refer to plasmids presumed to be inside the respective compartment: extracellular medium, cytoplasm, and nucleus. A mathematical representation of the three-compartment model was prepared that accommodated the experimentally measured outcomes, using data from the first 12 h of the experiment, beginning with plasmid introduction.

Mathematical compartmental model

Any mathematical model of a complicated biological system is a compromise among many factors including complexity, practicability, and utility. The three-compartment model reflects events that have biological significance, potentially limit nonviral transgene expression, and are experimentally measurable. In order to have a practical experimental model that measures important characteristics, some biological details may be intentionally excluded from experimental measurements. For this reason, the model and the corresponding mathematical representation used a 'lumped-parameter' approach that combined multiple biological events into a single mechanistic step. For example, plasmid DNA presumably crosses the cellular membrane using multiple methods, including passive diffusion, active transport via endocytosis, and receptor-mediated entry. The action of entry into the cell via any/all methods was 'lumped' into one rate constant that represented entry into the cell.

Similar combinations were applied for cytoplasmic transport and nuclear entry. Since the fate of plasmids inside the cell has not yet been precisely defined, and entry into the nucleus through the nuclear envelope is not well understood, these parameters were combined into a single rate constant that represented the rate of entry into the nucleus.

The following compartmental model was based on the concepts of mass action kinetics. Mass action kinetics describes the movement of mass through a system with translocation between compartments based on the concentration gradient and controlled by a proportionality rate constant. It was these rate constants that the mathematical model sought to estimate to facilitate identification of rate-limiting events in nonviral gene therapy and to quantitatively compare variations in nonviral plasmid delivery techniques. Three different systems of equations used to mathematically describe the three-compartment model previously described (Figure 2) were prepared.

The first system of differential equations presumed influx and out-flux of plasmid at each barrier. Plasmid may be transported in either direction across a cell barrier, even if equilibrium is achieved. The first differential equation represented the change in the number of plasmids in the medium over time:

$$\frac{dM}{dt} = -k_1 M + k_2 C \tag{1}$$

The plasmid number in the medium at various times, t, was represented by M. The plasmid number in the cytoplasm, also a function of time, was represented by C. The cytoplasmic plasmid numbers were calculated as the difference between the average plasmid number in entire, intact cells and their corresponding, isolated nuclei. The rate constants control plasmid motion across the barrier in the direction of the arrows identified in Figure 2. The rate constant k_1 represented the rate of cytoplasmic entry of the plasmid; k_2 represented the rate of plasmid entering from the cytoplasm into the extracellular medium.

The same type of differential mass action equation was prepared for both the cytoplasm and the nuclear compartments, respectively:

$$\frac{dC}{dt} = k_1 M - k_2 C - k_3 C + k_4 N \tag{2}$$

$$\frac{dN}{dt} = k_3 C - k_4 N \tag{3}$$

The plasmid number in the nucleus was represented by N. The rate at which plasmids are translocated from the cytoplasm to the nucleus was k_3, and the reverse rate from the nucleus to the cytoplasm was k_4. Both rates are in terms of (hr^{-1}).

Equations (1)–(3) were modified to incorporate the volumes of the three compartments:

$$\frac{dV_m[M]}{dt} = -k_1 V_m[M] + k_2 V_c[C] \tag{4}$$

$$\frac{dV_c[C]}{dt} = k_1 V_m[M] - k_2 V_c[C] - k_3 V_c[C] + k_4 V_n[N] \tag{5}$$

$$\frac{dV_n[N]}{dt} = k_3 V_c[C] - k_4 V_n[N] \tag{6}$$

These equations reflected the change in the plasmid concentration in each compartment as functions of time, using the volumes of the medium, cytoplasm, and nucleus, represented by V_m, V_c, and V_n, respectively. The square brackets indicate concentration of plasmid in the compartment. For example, the concentration of plasmid in the medium was [M]. Rearrangement of Equations (4)–(6) yields

$$\frac{d[M]}{dt} = -k_1[M] + k_2 \frac{V_c}{V_m}[C] \tag{7}$$

$$\frac{d[C]}{dt} = k_1 \frac{V_m}{V_c}[M] - k_2[C] - k_3[C] + k_4 \frac{V_n}{V_c}[N] \tag{8}$$

$$\frac{d[N]}{dt} = k_3 \frac{V_c}{V_n}[C] - k_4[N] \tag{9}$$

In the cases where translocation of plasmid occurred against the concentration gradient, a factor besides just passive diffusion needed to be taken into account. A third system of equations accounted for active transport in addition to the passive diffusion reflected in the previous equations. The following model was not derived from previous equations, but can be related to these previous representations through further mathematical manipulation. The motive behind this newly formulated mathematical model was to redefine our system with respect to possible active transport. The change in plasmid number in the medium over time became

$$\frac{dV_m[M]}{dt} = -k_{diff}^{mc}([M] - [C]) - k_{act}^{mc}[M] \tag{10}$$

The rates were then in terms of $mm^3\,h^{-1}$. The rate constant, k_{diff}^{mc}, represented the passive diffusion rate of plasmid across the medium/cytoplasm, *mc*, barrier. The rate constant k_{act}^{mc} represented active plasmid transport across the *mc* barrier. Dividing by V_m yielded an equation in terms of concentration:

$$\frac{d[M]}{dt} = -\left(\frac{k_{diff}^{mc} + k_{act}^{mc}}{V_m}\right)[M] + \frac{k_{diff}^{mc}}{V_m}[C] \tag{11}$$

Solving for k_{diff}^{mc} and k_{act}^{mc} using Equations (7) and (11) yielded the following relationships among the rate constants in the mass action and transport models:

$$\frac{k_{diff}^{mc}}{V_c} = k_2 = K_4, \quad \frac{k_{act}^{mc}}{V_c} = k_1 \frac{V_m}{V_c} - k_2 = K_3 - K_4 \tag{12a,b}$$

These relations are also presented in Tables 1 and 2.

The same active plus passive transport model was applied to the nuclear compartment:

$$\frac{dV_n[N]}{dt} = k_{diff}^{cn}([C] - [N]) + k_{act}^{cn}[C] \tag{13}$$

$$\frac{d[N]}{dt} = \left(\frac{k_{diff}^{cn} + k_{act}^{cn}}{V_n}\right)[C] - \frac{k_{diff}^{cn}}{V_n}[N] \tag{14}$$

Table 1 Volumetric rate constants

$K_1 = k_1$	
$K_2 = k_2\left(\frac{V_c}{V_m}\right)$	
$K_3 = k_1\left(\frac{V_m}{V_c}\right)$	
$K_4 = k_2$	
$K_5 = k_3$	
$K_6 = k_4\left(\frac{V_n}{V_c}\right)$	
$K_7 = k_3\left(\frac{V_c}{V_n}\right)$	
$K_8 = k_4$	

K_i in the left column are volumetric rate constants calculated from the k_i rate constants in the right column, also shown in Figure 2 (h^{-1}). V_i are compartment volumes.

Table 2 Active transport and passive diffusion rate constants calculation

$\frac{k_{act}^{mc}}{V_c} = k_1\frac{V_m}{V_c} - k_2 = K_3 - K_4$	
$\frac{k_{diff}^{mc}}{V_c} = k_2 = K_4$	
$\frac{k_{act}^{cn}}{V_n} = k_3\frac{V_c}{V_n} - k_4 = K_7 - K_8$	
$\frac{k_{diff}^{cn}}{V_n} = k_4 = K_8$	

Active and passive transport rate constants shown in the left column are calculated from the k_i rate constants in the center column and shown in Figure 2 (h^{-1}). V_i are compartment volumes. The right column provides the corresponding volumetric rate constant relations (K_i).

These equations yielded the diffusive and active rate constants, k_{diff}^{cn} and k_{act}^{cn}, for the cytoplasm/nuclear, *cn*, barrier:

$$\frac{k_{diff}^{cn}}{V_n} = k_4 = K_8, \quad \frac{k_{act}^{cn}}{V_n} = k_3\frac{V_c}{V_n} - k_4 = K_7 - K_8 \qquad (15a,b)$$

These rate constants can be compared quantitatively among experiments and can be used to evaluate the modulation of barrier rates by manipulation of experimental variables (Tables 3 and 4).

Computational compartmental model

The compartmental model was programmed in MatLab (The MathWorks, Inc., Natick, MA, USA). The plasmid numbers in each compartment at each time point were input as vectors. The MatLab function 'lsqnonlin' used a least-squares method to optimize the rate constants in the first system of differential equations as described previously in Equations (1)–(3). Optimum estimates of the rate constants were then used to calculate the volume-dependent rates of Equations (7)–(9). Additional composite rate constants, *K*, defined in Table 1, were also calculated from the initially obtained optimized rates.

Table 3 Estimated rate constants from the model

Rates (h^{-1})	*HeLa*	*CV1*
k_1	7.45E−04	4.71E−05
k_2	1.24E+00	3.44E−01
k_3	6.68E−01	9.48E−02
k_4	4.50E−01	7.99E−02
K_1	7.45E−04	4.71E−05
K_2	4.95E−04	6.84E−05
K_3	1.87E+00	2.37E−01
K_4	1.24E+00	3.44E−01
K_5	6.68E−01	9.48E−02
K_6	8.20E−03	1.40E−03
K_7	3.68E+01	5.23E+00
K_8	4.50E−01	7.99E−02

The first four rate constants are estimated from experimental data using the mathematical and compartment models shown as Equations (1)–(3) and Figure 2, respectively. The remaining eight volumetric rate constants (K_i) are calculated as indicated by the relations summarized in Table 1.

Table 4 Active transport and passive diffusion rate constants

Rates (h^{-1})	*HeLa*	*CV1*
$\frac{k_{diff}^{mc}}{V_c}$	1.24	0.34
$\frac{k_{act}^{mc}}{V_c}$	0.63	−0.11
$\frac{k_{diff}^{cn}}{V_n}$	0.45	0.08
$\frac{k_{act}^{cn}}{V_n}$	36.4	5.15

Active and passive rate constants for plasmid translocation across the cell membrane and nuclear envelope barriers are calculated as indicated by the relationships summarized in Table 2.

The diffusive and active rate constants are then found from the previous work by using Equations (11) and (14). These constants are presented in terms of volumes to facilitate comparison among experiments. The relations between these rates and those in Table 1 are shown in Table 2. These rate constants should help optimize the desired expression of the plasmid DNA in cells by quantifying the passage of plasmid DNA across the various cell barriers.

Acknowledgements

This work was supported by the Bioengineering and Environmental Systems Division of the National Science Foundation under Award BES-9902697. We would also like to acknowledge MB James for use of her experimental data on nonviral gene delivery and Dr MI Miga for reviewing this work.

References

1 Phillips AJ. The challenge of gene therapy and DNA delivery. *J Pharm Pharmacol* 2000; **53**: 1169–1174.

2 Leopold PL. Fluorescence methods reveal intracellular trafficking of gene transfer vectors: the light toward the end of the tunnel. *Mol Ther* 2000; **1**: 302–303.
3 Schatzlein AG. Nonviral vectors in cancer gene therapy: principles and progress. *Anticancer Drugs* 2001; **12**: 275–304.
4 Escrious V *et al*. Cationic lipid-mediated gene transfer: analysis of cellular uptake and nuclear import of plasmid DNA. *Cell Biol Toxicol* 1997; **14**: 95–104.
5 Lechardeur D *et al*. Metabolic instability of plasmid DNA in the cytosol: a potential barrier to gene transfer. *Gene Therapy* 1999; **6**: 482–497.
6 Capecchi MR. High efficiency transformation by direct microinjection of DNA into cultured mammalian cells. *Cell* 1980; **22**: 479–488.
7 Boussif O *et al*. A versatile vector for gene and oligonucleotide transfer into cells in culture and *in vivo*: polyethyleneimine. *Proc Natl Acad Sci* 1995; **92**: 7297–7301.
8 Farhood H, Serbina N, Huang L. The role of dioleoyl phosphatidylethanolamine in cationic liposome mediated gene transfer. *Biochim Biophys Acta* 1995; **1235**: 289–295.
9 Rakhmilevich AL *et al*. Cytokine gene therapy of cancer using gene gun technology: superior antitumor activity of interleukin-12. *Hum Gene Ther* 1997; **8**: 1303–1311.
10 Canatella PJ, Prausnitz MR. Prediction and optimization of gene transfection and drug delivery by electroporation. *Gene Therapy* 2001; **8**: 1464–1469.
11 Taniyama Y *et al*. Development of safe and efficient novel nonviral gene transfer using ultrasound: enhancement of transfection efficiency of naked plasmid DNA in skeletal muscle. *Gene Therapy* 2002; **9**: 372–380.
12 Liu F, Song YK, Liu D. Hydrodynamics-based transfection in animals by systemic administration of plasmid DNA. *Gene Therapy* 1999; **6**: 1258–1266.
13 Cartier R *et al*. *In vivo* gene transfer by low-volume jet injection. *Anal Biochem* 2000; **282**: 262–265.
14 Pouton CW, Seymour LW. Key issues in non-viral gene delivery. *Adv Drug Deliv Rev* 1998; **34**: 3–19.
15 Plank C, Zauner W, Wagner E. Application of membrane-active peptides for drug and gene delivery across cellular membranes. *Adv Drug Deliv Rev* 1998; **134**: 21–35.
16 Fajac I, Briand P, Monsigny M, Midoux P. Sugar-mediated uptake of glycosylated polylysines and gene transfer into normal and cystic fibrosis airway epithelial cells. *Hum Gene Ther* 1999; **10**: 395–406.
17 Zabner J *et al*. Cellular and molecular barriers to gene transfer by a cationic lipid. *J Biol Chem* 1995; **270**: 18997–19007.
18 Brunner S *et al*. Cell cycle dependence of gene transfer by lipoplex, polyplexes and recombinant adenovirus. *Gene Therapy* 2000; **7**: 401–407.
19 Tseng W-C, Haselton FR, Giorgio TD. Mitosis enhances transgene expression of plasmid delivered by cationic liposomes. *Biochim Biophys Acta* 1999; **1445**: 53–64.
20 Ledley TS, Ledley FD. Multicompartment, numerical model of cellular events in the pharmacokinetics of gene therapies. *Hum Gene Ther* 1994; **5**: 679–691.
21 Varga CM, Hong K, Lauffenburger DA. Quantitative analysis of synthetic gene delivery vector design properties. *Mol Ther* 2001; **4**: 438–446.
22 James MB, Giorgio TD. Nuclear-associated plasmid, but not cell-associated plasmid, is correlated with transgene expression in cultured mammalian cells. *Mol Ther* 2000; **1**: 339–346.
23 Chan CK, Jans DA. Using nuclear targeting signals to enhance nonviral gene transfer. *Immunol Cell Biol* 2002; **80**: 119–130.
24 Nakanishi M *et al*. Nuclear targeting of DNA. *Eur J Pharm Sci* 2001; **13**: 17–24.
25 Panté N, Kann M. Nuclear pore complex is able to transport macromolecules with diameters of ~39 nm. *Mol Biol Cell* 2002; **13**: 425–434.
26 Stewart M. Nuclear pore structure and function. *Semin Cell Biol* 1992; **3**: 267–277.
27 Welz C *et al*. Nuclear transport of oligonucleotides in HepG2-cells mediated by protamine sulfate and negatively charged liposomes. *Pharm Res* 2000; **17**: 1206–1211.